Biol. Chem., Vol. 386, pp. 833–844, September 2005 • Copyright © by Walter de Gruyter • Berlin • New York. DOI 10.1515/BC.2005.098

Review

Symmetry at the active site of the ribosome: structural and functional implications*

Ilana Agmon, Anat Bashan, Raz Zarivach and Ada Yonath**

Department of Structural Biology, The Weizmann Institute, 76100 Rehovot, Israel

**Corresponding author
e-mail: ada.yonath@weizmann.ac.il

Abstract

The sizable symmetrical region, comprising 180 ribosomal RNA nucleotides, which has been identified in and around the peptidyl transferase center (PTC) in crystal structures of eubacterial and archaeal large ribosomal subunits, indicates its universality, confirms that the ribosome is a ribozyme and evokes the suggestion that the PTC evolved by gene fusion. The symmetrical region can act as a center that coordinates amino acid polymerization by transferring intra-ribosomal signals between remote functional locations, as it connects, directly or through its extensions, the PTC, the three tRNA sites, the tunnel entrance, and the regions hosting elongation factors. Significant deviations from the overall symmetry stabilize the entire region and can be correlated with the shaping and guiding of the motion of the tRNA 3′-end from the A- into the P-site. The linkage between the elaborate PTC architecture and the spatial arrangements of the tRNA 3′-ends revealed the rotatory mechanism that integrates peptide bond formation, translocation within the PTC and nascent protein entrance into the exit tunnel. The positional catalysis exerted by the ribosome places the reactants in stereochemistry close to the intermediate state and facilitates the catalytic contribution of the P-site tRNA 2′-hydroxyl.

Keywords: peptide bond formation; ribosome structure and function; ribosomal symmetrical region; rotatory mechanism.

Introduction

The ribosome is the universal cellular assembly that translates the genetic code into proteins. Ribosomes from all living cells consist of two riboprotein subunits of unequal size that associate upon the initiation of protein biosynthesis and dissociate once this process is terminated. The small ribosomal subunit facilitates the initiation of the translation process and is involved in selecting the correct translated frame, in decoding the genetic message and in controlling the fidelity of codon-anticodon interactions. The large ribosomal subunit catalyzes peptide bond formation and guarantees the elongation of nascent proteins by channeling them into the exit tunnel. Protein biosynthesis is performed cooperatively by the two ribosomal subunits and several non-ribosomal factors. Since cell vitality requires fast and smooth processing of protein formation, the ribosome possesses features allowing transmission of signals between its various functional sites.

mRNA brings the genetic instructions to the ribosome and aminoacylated tRNA molecules deliver the amino acids in a ternary complex with elongation factor Tu-GTP (EF-Tu-GTP). All tRNA molecules have a similar L-shape structure, and although they are built primarily of double helices, single-stranded regions host their functional sites. The tRNA anticodon stem loop performs the decoding by base-pairing with the mRNA, and its 3′-end, a nucleotide quartet ending with a triplet of the universal sequence CCA, carries the amino acids. The ribosome possesses three tRNA binding sites, each located on both subunits. The A-site hosts the aminoacylated tRNA, the P-site is the location of the peptidyl tRNA, and the E-site designates the position of the exiting deacylated tRNA. The elongation of the polypeptide chain is associated with A→P→E translocation of the mRNA, together with the tRNA molecules bound to it. In each cycle of the elongation event, a new peptide bond is formed. The peptidyl chain is detached from its tRNA and the deacylated tRNA molecule exits the ribosome through the E-site, while the A-site tRNA is translocated to the P-site.

The currently available three-dimensional structures of ribosomal particles (Ban et al., 2000; Schluenzen et al., 2000; Wimberly et al., 2000; Harms et al., 2001; Yusupov et al., 2001) revealed that the interface surfaces of both subunits are rich in RNA, and that only one ribosomal protein, S12, is involved in decoding at the small subunit. The peptidyl transferase center (PTC) in the large subunit, where peptide bonds are formed, consists exclusively of ribosomal RNA, confirming that the ribosome is a ribozyme, as suggested based on biochemical results obtained over a decade ago (Noller et al., 1992).

A sizable symmetrical region in the asymmetric ribosome and its internal architecture

In previous studies (Agmon et al., 2003, 2004; Bashan et al., 2003a,b; Yonath, 2003a,b; Zarivach et al., 2004) we established the existence of a sizable region related by a local two-fold symmetry (SymR) in and around the PTC. This region contains approximately 180 nucleotides and is present in all known structures of the large ribosomal

* This article is published in connection with the Fritz-Lipmann-Lecture, delivered by Ada Yonath at the Annual Fall Meeting of the German Society for Biochemistry and Molecular Biology (GBM) in Berlin, September 2005.

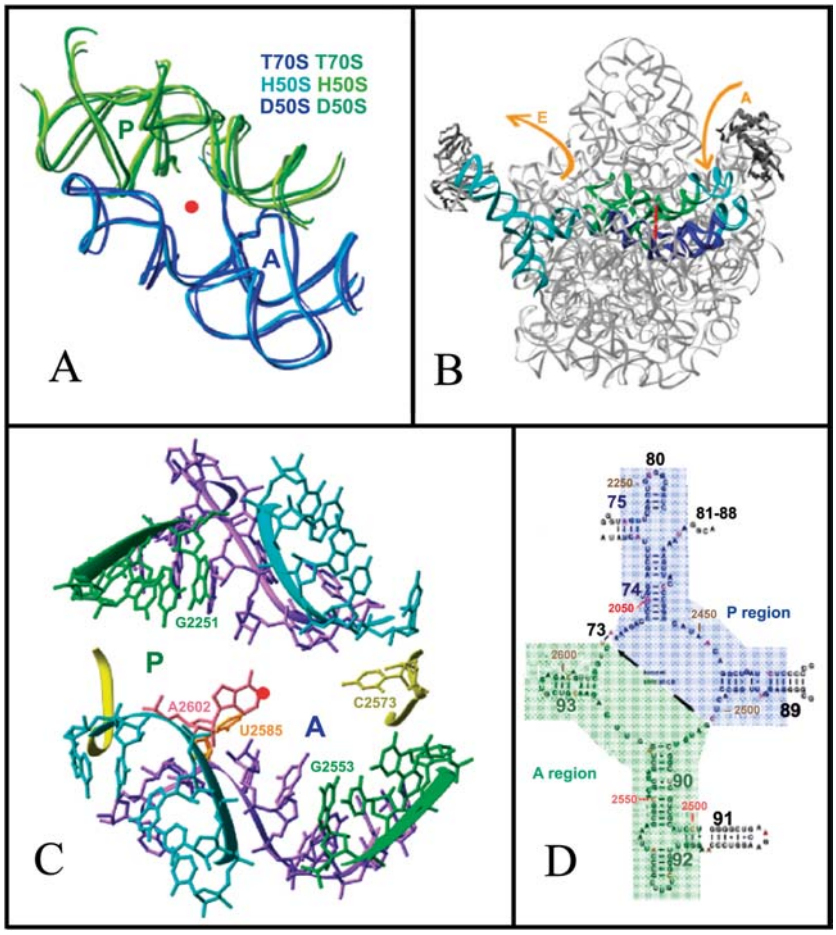

Figure 1 The symmetrical region in the structure of the large ribosomal subunit.
(A) Overlap of the backbone fold of D50S (PDB 1NKW), H50S (PDB 1JJ2) and T70S (PDB 1GIY). (B) The location of the SymR (A-region in blue, P-region in green), three of its non-symmetrical extensions (in cyan) and the two-fold symmetry axis (in red) within the large ribosomal subunit of D50S (represented by the backbones of its 23S and 5S RNA chains, shown as gray ribbons). The two orange arrows indicate the approximate directions of the incoming A-site and E-site tRNA (A and E, respectively). (C) The inner part of the SymR. Shown are nucleotides within 15 Å from the two-fold symmetry axis, marked by a red circle. Related elements are identically colored. The rear wall is situated between the A- and the P-loop, opposite to A2602. Upper PTC rims constructed of the A-, P-loops (in green) and of the inner strands of helix H89, helix H93 (in cyan) distinctly obey the symmetry. The C-loop segments H74–89 and H90–93 (in purple) and the mismatch zone (shown, except from C2573, by its backbone colored in yellow) show less symmetry conservation. (D) The secondary structure scheme of the SymR derived from the D50S crystal structure (Harms et al., 2001), drawn in a manner that exhibits the two-fold symmetry of the region (*E. coli* and D50S numbering in gray and red, respectively). Note that the symmetry relates helix H74 to helix H90, the three base pairs at the beginning of helices H75 and H91, helix H80 to helix H92, about half of helix H89 to helix H93, and the loops between the helices. In the C-loop it relates H74–89 to H90–93, and H89–H90P (part of H89–90 that belongs to the P-region, as defined in Figure 2) to H93–73. H73–74, however, is displaced due to the existence of H73 and is not compatible with H89–90A.

subunit (Figure 1A), namely the eubacterium *Deinococcus radiodurans*, D50S, the archaeon *Haloarcula marismortui*, H50S, and their complexes with ligands and substrate analogs (Ban et al., 2000; Nissen et al., 2000; Harms et al., 2001; Hansen et al., 2002; Schmeing et al., 2002; Bashan et al., 2003a), and the complex of the thermopile *T. thermophilus* ribosome, T70S, with three tRNA molecules (Yusupov et al., 2001). The SymR extends far beyond the vicinity of the peptide synthesis location. It interacts, directly or through the extensions of its helices, with features of utmost importance to the ribosome function, such as the two large subunit stalks that serve as the entrance and exit points of A- and E-site tRNA (Figure 1B). The SymR local symmetry axis passes through the peptidyl transferase center, midway between the A- and P-loops (Figure 1C) and is directed into the protein exit tunnel.

The secondary structure scheme of the SymR, derived from the D50S crystal structure (Harms et al., 2001) and modified to exhibit the two-fold symmetry detected at the three-dimensional level, is shown in Figure 1D. This scheme demonstrates that the SymR is composed of RNA helices radiating from the central loop of domain V (C-loop), and can be divided into two sub-regions. The A-region spans from nucleotide G2502 (numbering and nucleotide type used according to the *E. coli* system throughout) to C2610 on the C-loop, and its symmetry-related P-region ranges from nucleotide A2058 to C2501 on this loop. A list of all the nucleotides of the SymR, their symmetry relations, and information concerning their secondary structure and phylogenetic conservation, is given in Figure 2. This Figure, as well as the structural observations given below, equally corresponds to the structures of D50S and H50S, unless stated otherwise.

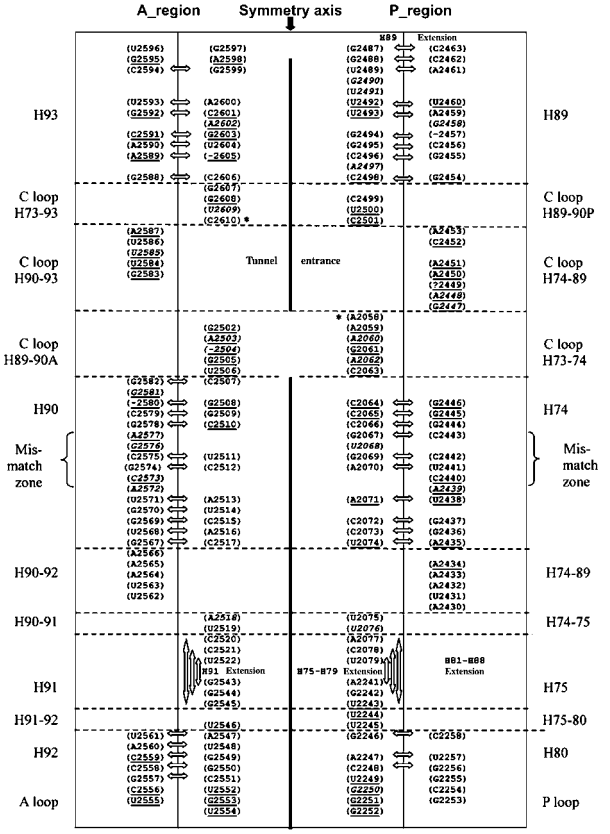

Figure 2 All SymR nucleotides.
The first and last nucleotides in the region are marked by asterisks. The central vertical line represents the two-fold symmetry axis, relating the A- and P-region nucleotides that lie on the same row. Differences in the number of nucleotides in related structural elements may occasionally lead to an uncertainty of ±1 in the assignment of symmetrical mates, as shown in Figure 2B. Symmetry is obeyed between all related nucleotides unless bulged (indicated by letters in italics), or located at areas where the line symbolizing the two-fold symmetry axis is erased (i.e., between H73–74 and H89–90A in the C-loop and between G2595–2596 from the stem loop of H93, which do not fit C2462–2463 of the H89 stem). Base-paired nucleotides are connected by arrows. The arrows symbolizing base pairs in H75 and its related H91 are vertical because of the H74-H75-H80 junction. Nucleotides that are more than 98% conserved are underlined (Cannone et al., 2002).

To define the quantitative correlation between these two subregions, the D50S A-region was overlapped onto the P-region. The best match, i.e., a minimal root mean square deviation between the overlapping entities, was obtained when the A-region was rotated by 179.6° around an axis termed the symmetry axis of the SymR, thus indicating two-fold symmetry. The match between the backbone folds is evident from the superposition of the P-region and the 180°-rotated A-region, as shown in Figure 3A. Conformational compatibility between individual nucleotides and their 180° rotation-related matches (Figure 3B) indicates that the symmetry applies to the RNA backbone fold as well as to nucleotide conformation.

The inner part of the SymR is a conical pocket, with the A- and the P-loops residing on its opposite sides and the polypeptide exit tunnel emerging from its bottom. The wall of this pocket that extends from the A- to the P-site and is located closer to the intersubunit interface is called here the front wall. Together with the opposite wall (the rear wall), it creates an inner void whose upper rims are formed by the A- and P-loops and by the inner strands of helices H89 and H93 (nucleotides U2492–2498, A2600–2606, respectively). Beneath are the C-loop segments H74–89 (namely the loop segment between helices H74 and H89) and H90–93 (namely the loop segment between helices H90 and H93) and several nucleotides from helices H74 and H90, which demonstrate less symmetry than the upper rims (Figure 1C). The bottom of the pocket that forms the tunnel entrance consists of nucleotides from the C-loop segments H73–74 and H89–90A (defined in Figure 2) that do not comply with the two-fold symmetry, indicating that the symmetry ceases to be obeyed at a height corresponding to the tunnel entrance.

The RNA backbones of the A- and P-regions interact with each other only at two locations, both at the tunnel entrance. One is the bond between nucleotides C2501 and G2502, i.e., between H89–90P and H89–90A (the two parts of the loop section between helices H89 and H90, belonging to the P- and A-region, respectively). The other contact, between H73–74 and H93–73, is mediated by helix H73 (Figures 1D and 3C). Nucleotides from the A- and P-regions intermingle at the bottom of the PTC, whereas only sporadic contacts occur between the upper parts of the A- and P-regions. As discussed below and shown in Figure 3C, the number of interactions between the two sides of the A- and P-regions are significantly unbalanced.

The symmetry-related region interacts with major functional sites

The SymR extends to a distance of approximately 40 Å from the PTC midpoint (Figure 1B). Its location within the large subunit allows direct or indirect interactions with almost all large ribosomal-subunit components possessing functional relevance and with all the factors involved in the elongation process. The 3′-ends of the A- and P-tRNAs bind to the PTC, whereas the 3′-end of the E-site tRNA contacts the neighborhood of nucleotide A2433 at the edge of the SymR in the structure of T70S complexed with three tRNA molecules (Yusupov et al., 2001), but not in the structure of H50S complexed with E-site tRNA (Schmeing et al., 2003). The non-symmetrical extensions radiating from the SymR interact with regions that carry out central roles in the ribosome function. These include the part of the L1 arm that is involved in the release of E-site tRNA from the ribosome, namely helices H76–8 (Figure 1B) that extend from helix H75 of the SymR; the extension comprised of helices H81–H88 that reaches 5S rRNA; helix H89 extension (Figure 1B), whose stem-loop nucleotide G2485 interacts with nucleotide C1092 of helix H44, in a region implicated in binding of the ternary complex (Simonson and Lake, 2002) and in GTPase activity (Wimberly et al., 1999; Valle et al., 2002); and H91 extension (Figure 1B), whose stem loop nucleotides A2531 and G2532 interact with nucleotides A2662 and G2663 of the sarcin-ricin loop of H95, which accommodates EF-Tu and EF-G (Hausner et al., 1987; Moazed et al., 1988; Wilson and Noller, 1998; Wriggers et al., 2000; Mohr et al., 2002; Stark et al., 2002).

No direct contact is found between the SymR of D50S and the small subunit 30S, based on docking (Bailey,

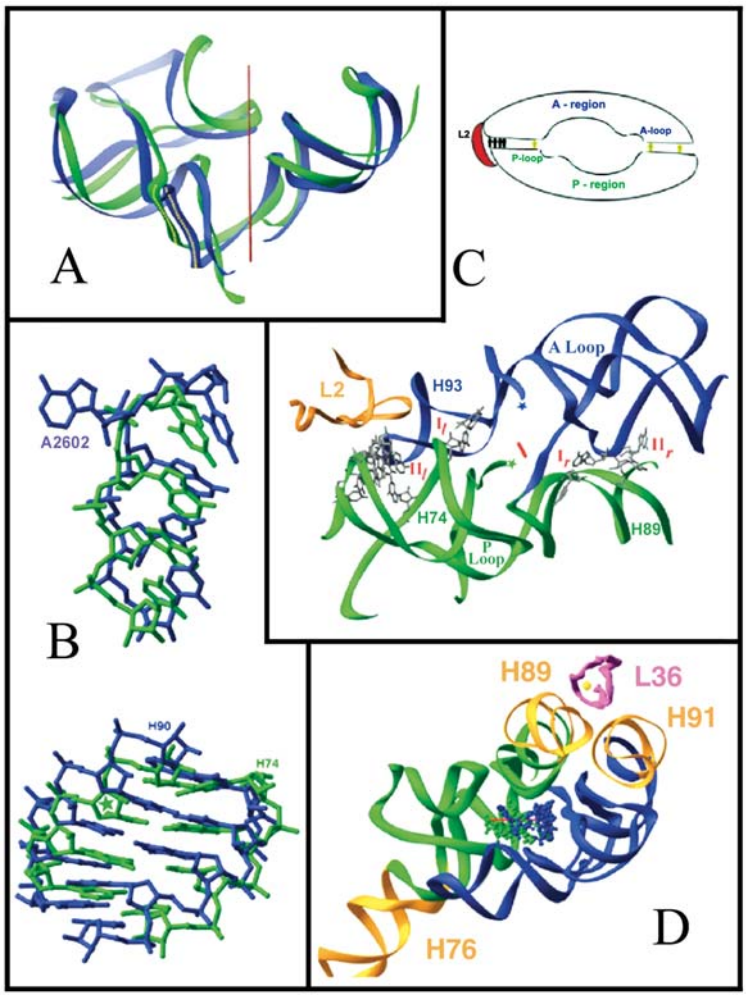

Figure 3 Relationships between the A- and P- regions.
(A) The match between backbone folds of the P-region and of the 180°-rotated A-region, shown by superposition of the two regions. The mismatched zone is indicated by yellow dots. The symmetry operation that relates the A- to the P-region was determined using the program LSQKAB (Bailey, 1994). All 22 base pairs that have symmetry-related mates (Figure 2), forming a subset of the 25 base pairs that compose each of the A- and the P-regions of D50S, were overlapped for both the native structure of D50S (Harms et al., 2001) and for ASM-D50S (Bashan et al., 2003a). The transformation matrix indicated two-fold symmetry, related by an axis termed 'the symmetry axis of the SymR', with direction cosines given by (0.95, 0.08, -0.32). (B) Conformational compatibility between nucleotides of the P-region and of the 180°-rotated A-region: overlap of nucleotides located around the bulged A2602 and their related ones and the overlap between related parts of helices 74 and 90. H74 nucleotide marked by an asterisk (in green) can be related to either one of the two neighboring H90 nucleotides above or below it (in blue), demonstrating a case of uncertainty in assigning symmetry-related nucleotides. (C) Top: a scheme demonstrating the A- to P-region interactions. Yellow and black arrows denote A- to P-region contacts, which involve and do not involve bulged nucleotides, respectively. The lune represents L2, which interacts with both the A- and P-regions. Bottom: the A- to P-region interactions in the structure of D50S (Harms et al., 2001), viewed approximately from the tunnel direction. Note that the backbones of the A- and the P-regions interact at two locations at the tunnel entrance: directly, at the middle of H89–90 loop (the meeting point of the green and blue ribbons), and mediated by H73, for which the position of the first base pair is marked by asterisks. Most of the RNA is represented by its backbone, but the nucleotides involved in interactions between the upper rims of the A- and P-regions are fully shown. Note the differences between the two sides. On the SymR right-hand side, two contacts are formed between bulged nucleotides (marked by Ir,IIr). In contrast, one such contact (II) and a large connectivity network of non-bulged nucleotides (marked by II) exist on the left side. Protein L2 interacts with both regions at the far left-hand side. (D) The interactions of protein L36 (in magenta, the yellow circle denotes the Zn position) with the non-symmetrical extensions H89 and H91 (in gold) of the SymR (A-region in blue, P-region in green).

1994) the T70S structure (Yusupov et al., 2001). Signal transmission between the SymR and the small subunit can be mediated by several features, including the inter-subunit bridges (Yusupov et al., 2001). These include helix H68 (bridge B7a) and helix H71 (bridge B3), the loop segments H69–71 and H67–71, protein L2 (bridge B7b), which was previously suggested to serve as a relay between the small subunit and the catalytic center in the large one (Uhlein et al., 1998), protein L14 (bridge B8), and A- and P-site tRNAs.

The loop segments H69–71 and H67–71 can also communicate between helix H69, the major component of the B2a bridge that reaches the vicinity of the decoding center in the small subunit and the SymR (Yusupov et al., 2001). Thus, the spatial organization of this region seems to enable transmission of signals between these remote locations on the ribosome (Agmon et al., 2003). The outer SymR shell interacts, directly or through its extensions, with all the substrates and factors involved in the elongation stage, while its inner part hosts the pep-

tide bond formation site and the entrance to the exit tunnel. Hence, it is likely that the SymR functions as the center of coordination for protein biosynthesis, a process depending on synchronization between many factors and ribosomal components. The finding of a symmetry-related region around the ribosomal active site in two of the three kingdoms of life, i.e., in bacteria and archaea, is consistent with the universality of the protein biosynthesis process.

A symmetrical arrangement of the PTC allows the reactants involved in peptide bond formation to be positioned in favorable stereochemistry, namely facing each other. This, together with the requirement to provide the two chemically equivalent 3′-ends at the A- and P-sites with two comparable supportive environments, justifies the existence of a region related by two-fold symmetry. In accordance with the suggestion that the symmetry serves the accommodation of the tRNA termini, it terminates below the 3′-ends, i.e., at the tunnel entrance.

Proteins at the rims of the symmetrical region

No proteins are present in the SymR of the D50S structure, but proteins L2, L3, L14, L16 and L31 embrace the region from its exterior. In H50S, L10e replaces L16 and the contacts of L31 with the SymR in D50S are replaced by interactions with two H50S proteins – L15e and L44e (Harms et al., 2001). The contacts made by the SymR with L4, L13, L27 and L32 exist solely in the D50S structure, whereas only in the H50S structure do the N-terminus residues of L3, penetrating towards the A-loop (Klein et al., 2004), interact with the SymR. Interestingly, L2 is the only protein that interacts with both the A- and P-regions. Its contacts with the P-region in the D50S structure, taking place via residues 228 and 229. The latter was shown to be essential for processing of peptidyl transferase activity (Cooperman et al., 1995), namely for elongation of the nascent chain, although the entire protein is not required for the formation of a single peptide bond (Nitta et al., 1998).

Involvement in peptidyl transferase activity can also be attributed to protein L36, which in D50S is situated in the middle of four parallel helices: H42, H97 and the non-symmetrical extensions of helices H89 and H91. Each of the four helices surrounding L36 is directly interconnected with its two neighboring helices. Nevertheless, L36 interactions with all of them can further glue the helices together. Three of these helices, H42, H89 and H91, interact via helices H44 and H95 with the binding sites of the elongation factors. Hence it is conceivable that this region is involved in chaining information about factor binding through helices H89 and H91 (Figure 3d) into the PTC, presumably for triggering the conformational alterations required for different steps of protein biosynthesis. The availability of alternative routes for signaling and of alternative means for conformation preservation, through the non-symmetrical extensions of the SymR, may account for the absence of L36 in some species, such as *H. marismortui.*

Breaking of the two-fold symmetry

Whereas the overall spatial organization of the SymR complies with the two-fold symmetry (Figure 3A,B), there is no overall sequence identity between related nucleotides in the A- and P-regions. Moreover, a considerable proportion of the nucleotides within the region exhibits significant diversion from the symmetry, occurring at several levels.

Symmetry breaking at the nucleotide conformation level

The SymR contains more than 20 bulged nucleotides, some of them sticking out from helices and others from loops. Bulged nucleotides do not overlap significantly with their neighboring nucleotides (Figure 3B) and can therefore possess considerable flexibility. No bulged nucleotide in the SymR obeys the symmetry, in contrast to the pronounced symmetry preservation among the non-bulged nucleotides. In a few cases the bulged nucleotide has a two-fold related mate with a completely different conformation, but mostly they have no mates (Figure 2). In addition, bulged nucleotides tend to locally disrupt the fold and conformation of their neighboring nucleotides. An example is a ‘mismatch zone’ in helix H74 and its related helix H90, defined in Figure 2, which contains a large number of bulged nucleotides, causing a twist in the backbone fold and altering the kink direction (Figures 1C and 3A). These observations characterize nucleotide bulging as a major cause of symmetry breaking in the SymR.

The bulged nucleotides in the SymR can be categorized according to their topology (Table 1). The first subgroup includes nucleotides that stick outwards and interact with the other features of the ribosome. Some of these nucleotides, such as G2250, may be involved in stabilizing specific areas of the SymR. Others may contribute to the communication pathways between the inner part of the SymR, where the peptide bond is being formed, and the ribosome periphery, involved in the accommodation and release of the factors. The second subgroup in Table 1 contains nucleotides that bulge inwards the SymR bulk. Most of these nucleotides seem to participate in internal stabilization of the SymR, either by forming base pairs and stacking interactions to proximal, albeit sequentially remote nucleotides within the region, or by forming contacts between the A- and the P-regions at the upper and bottom edges of the PTC. The third and seemingly most important subgroup consists of bulged nucleotides that interact with the substrates and product of peptide synthesis, i.e., with the tRNA 3′-ends and the nascent peptide. A detailed description of the presumed task of each nucleotide in this group is given below, while discussing the rotatory mechanism.

Symmetry breaking in the network of A- to P-region contacts

As indicated above, the backbones of the A- and P-regions are directly bonded at only two points, both at the tunnel entrance (Figures 1D and 3C). This may confer mobility to the upper rims of the PTC. Hydrogen bonds form additional interconnections (Figure 3C) between the upper parts of the PTC, and although the helices involved in the interactions mostly obey the symmetry, many of the connecting hydrogen bonds do not. This apparent

Table 1 The SymR bulged nucleotides, their phylogenetic conservation and the direction of their bulged bases.

Nucleotide	Position	Conservation (%)[a]	Bulged towards
Bulging outwards of the SymR			
A2060	C loop, H73–74	100	H26-46 loop. Also stacked against G2502 (C loop, H89–90A)
G2250	P loop	97	L16 (L10e in H50S) in D50S is involved in ASM remote interactions, suggested to govern accurate substrate positioning (Bashan et al., 2003a)
A2448	C loop, H74–89	97	H37-38 loop
A2577	H90 MZ	100	Nucleotides G2056, A2614 from the two strands of H73 at the upper part of the tunnel
Forming intra-region contacts			
U2068	H74	93[b]	A2430 (C loop, H74–89), to which it is base-paired
U2076	H74–75	None	U2596 (H93 stem loop), forming an A- to P-region interaction
A2439	H74	98	Forming through its ribose an A- to P-region, contact with U2586 (C loop, H90–93)
G2447	C loop, H74–89	98	Stacked between U2500, C2501 (C loop, H89–90P), forming (in D50S) a hydrogen bond to U2504 at the bottom of the PTC
G2458	H89	<80	The core of H89; stacked against G2490
G2490	H89	83	The core of H89; stacked against G2458
U2491	H89	93	Forming an A- to P-region contact to G2570 (H90) through its ribose
A2497	H89	84	The phosphates of A2450,1
A2503	C loop, H89-90A	98	Stacked between A2059, G2061 (C loop, H73–74), at the bottom of the PTC
U2504	C loop, H89-90A	98	Forming an A- to P-region contact with A2572 (H90) through its ribose
A2518	H90-91	93	U2489 (H89), forming an A- to P-region contact (in H50S)
A2572	H90 MZ	97	U2504 (C loop, H89-90A); also forms an A- to P-region contact with A2453 (C loop, H74-89) through its ribose
G2576	H90 MZ	98	Phosphate of U2506
G2581	H90	98	Phosphate of U2609
Interacting with the PTC substrates			
A2062	C loop, H73–74	97	Rotating amino acid (Agmon et al., 2003; Bashan et al., 2003a)
C2573	H90 MZ	100	Rotating CCA (Agmon et al., 2003; Bashan et al., 2003a)
U2585	C loop, H90–93	99	The PT center. Interacts with tip of A- and P-site tRNA 3′-ends (Nissen et al., 2000; Yusupov et al., 2001; Bashan et al., 2003a) and the rotating CCA; suggested to anchor the rotating moiety (Agmon et al., 2003; Bashan et al., 2003a)
A2602	H93	99	PT center; interacts with A- and P-site tRNA 3′-ends (Nissen et al., 2000; Yusupov et al., 2001; Bashan et al., 2003a) and the rotating CCA, in the vicinity of the connection to the tRNA acceptor stems; suggested to anchor the rotating moiety, assisting passage of the tRNA 3′-end from the A- to the P-site (Agmon et al., 2003; Bashan et al., 2003a)
U2609	C loop, H73–93	96	The tunnel's upper part; cross-links to the C terminus of the elongating peptide (Stade et al., 1995)

[a] Phylogenetic conservation across three phylogenetic domains and two organelles. Sample consisting of 930 species (Cannone et al., 2002).
[b] Missing in more than 10% of the species (Cannone et al., 2002).
MZ, mismatch zone.

contradiction results from the involvement of symmetry-breaking elements, such as bulged nucleotides and the stem loop of helix H93 (Figure 2), in the formation of all the upper A- to P-region contacts.

Although the interactions between the A- and P-regions in H50S and D50S (listed in detail in Table 2) are not identical, a common theme is retained (Figure 3C, top). On the right side of the SymR there are only two contacts, both formed by presumably flexible, bulged nucleotides. The far left-hand side, on the contrary, contains a network of A- to P-region contacts between non-bulged nucleotides, which apparently form a firm construction. In addition, protein L2, which interacts with both the A- and P-regions on the far left-hand side of the SymR in D50S and H50S, thus enhancing the A- to P-region contacts on that side, has no corresponding protein on the right-hand side. The unbalanced number of A- to P-region contacts between the two sides of the SymR (left and right as in Figure 3C) and the presumed flexibility of the bulged nucleotides forming all but the far left-hand side contacts may be related to the dynamics of the PTC. The involvement of L2 in the suggested SymR mobility is consistent with its high evolutionary conservation and with the key role L2 plays in tRNAs accommodation (Diedrich et al., 2000) as part of the elongation process as described above.

Symmetry breaking between the A- and P-sites

The related helices H80 and H92, whose stem loops accommodate the tRNA 3′-ends, show a low degree of compatibility between themselves. Helix H80 has three

Table 2 A- to P-region contacts.

SymR-left		SymR-right	
Interacting bases	Interaction symbol	Interacting bases	Interaction symbol
D50S			
A2439 (H74)-U2586 (H90–93)	I/	*A2572* (H90)-A2453 (H74–89)	I*r*
U2075 (H74–75)-U2596 (H93 stem loop) U2074 (H74)-G2597 (H93 stem loop) C2073 (H74)-A2598 (H93 stem loop) G2436 (H74)-A2598 (H93 stem loop)	II/	G2570 (H90)-*U2491* (H89)	II*r*
H50S			
A2439 (H74)-U2586 (H93)	I/	*A2518* (H90-91)-U2489 (H89)	I*r*
U2074 (H74)-G2597 (H93 stem loop) C2073 (H74)-A2598 (H93 stem loop) G2437 (H74)-G2599 (H93) A2439 (H74)-A2600 (H93)	II/	G2569 (H90)-*U2491* (H89)	II*r*

The structural elements of the nucleotides are given in parentheses. Bulged nucleotides are indicated by italic font. Left and right sides are assigned according to Figure 3C.

base pairs compared to five base pairs in the related helix H92, and its P-loop consists of seven nucleotides instead of five nucleotides in the A-loop (Figure 1D). Whereas A-loop nucleotides do not form any contacts with the ribosome outside the SymR, the P-loop nucleotide G2255 makes an out-of-SymR base pair with C2275 of helix H81 and the bulged P-loop nucleotide G2250 interacts with protein L16. The difference in the bonding scheme between the two loops and the firm contact between the A- and P-regions in the vicinity of the P-site (Figure 3C) seem to be correlated to the excess mobility of the A-site.

The rotatory motion

Consistent with the ribosomal symmetry, the tRNA termini were found to be related by a two-fold symmetry (Nissen et al., 2000; Yusupov et al., 2001; Hansen et al., 2002; Schmeing et al., 2002), whereas the stems of the A- and P-site tRNAs are related by a sideways shift (Stark et al., 1997; Agrawal et al., 2000; Yusupov et al., 2001). Indeed, symmetry relation between A76 of two tRNAs was detected independently even in a combined model of the structures of two H50S complexes, one with a compound that was supposed to resemble a reaction intermediate, and the second with a substrate analog of which the acceptor stem and nucleotide connecting it to the CCA end are disordered (Nissen et al., 2000). Furthermore, the ribosomal symmetrical frame was found to govern the overall positioning of the tRNA molecules, even in cases of semi-productive binding, requiring additional rearrangements to participate in peptide bond formation (Hansen et al., 2002). Accordingly, the universal Watson-Crick base pair between C75 of the A-site tRNA terminus (or its substrate analog equivalent) and G2553 (Kim and Green, 1999) was found to be related by the same symmetry to the base pair between C75 and G2251 at the P-site (Nissen et al., 2000; Yusupov et al., 2001; Hansen et al., 2002; Schmeing et al., 2002). This indicates that during translocation the A-site 3′-end moves into the P-site, where it is accommodated with an orientation facing its original one, by a 180° rotatory mechanism (Agmon et al., 2003; Bashan et al., 2003a) (Figure 4A). Furthermore, in the complex of D50S with ASM (a 35-ribonucleotide oligomer mimicking the aminoacylated-tRNA acceptor stem and its universal 3′-end), as well as in that of T70S with three tRNAs (Yusupov et al., 2001) docked onto D50S, the bond connecting the A-site 3′-end with the tRNA-acceptor stem was found to approximately coincide with the 180° rotation axis, suggesting that the tRNA terminus can go through this motion independently of the stem.

The A- to P-site rotation of the A-tRNA terminus has to be performed within the PTC, since during the motion the aa-3′-end is bonded to its acceptor stem from above and linked to the nascent chain from below (Figure 4A). In view of the size of the tRNA aa-3′-end, the only free space within the PTC that allows proper passage from the A- to the P-site dictates motion along the PTC rear wall (Figure 1C). The role of the PTC rear wall as a template for the translocating terminus is demonstrated by the spatial match between its nucleotides and the contour of the tRNA aa-3′-end, formed by the rotatory motion (Figure 4B,C) as well as by the extreme conservation of rear-wall nucleotides discussed below, including the fully conserved G2061 and C2573, which so far were not implicated in any other role.

The motion of the aa-3′-end from the A- to the P-site (Figure 4B,C) was simulated using the coordinates of ASM in its complex with D50S. As a result, C75 of the derived P-site tRNA terminus was found to form a base pair with G2251, which is symmetrical to the universal A-site C75-G2553 base pair (Bashan et al., 2003a). It appears, therefore, that passage of the A-site tRNA to the P-site involves two independent, albeit correlated, motions: a rotatory movement of approximately 180° of the tRNA termini from the A- to the P-site within the PTC, and a sideways shift of the A-tRNA helical regions into P, which is performed as a part of the overall mRNA/tRNA translocation. The rotatory and translatory components of the symmetry element that transforms the A-site terminus into the P-site were found to be composed of a 179° rotation and a 2-Å shift in the direction of the tunnel, implying an overall spiral motion (Figure 4B,C).

The PTC is an arched void confined by its rear wall and by two nucleotides that bulge from the front wall into

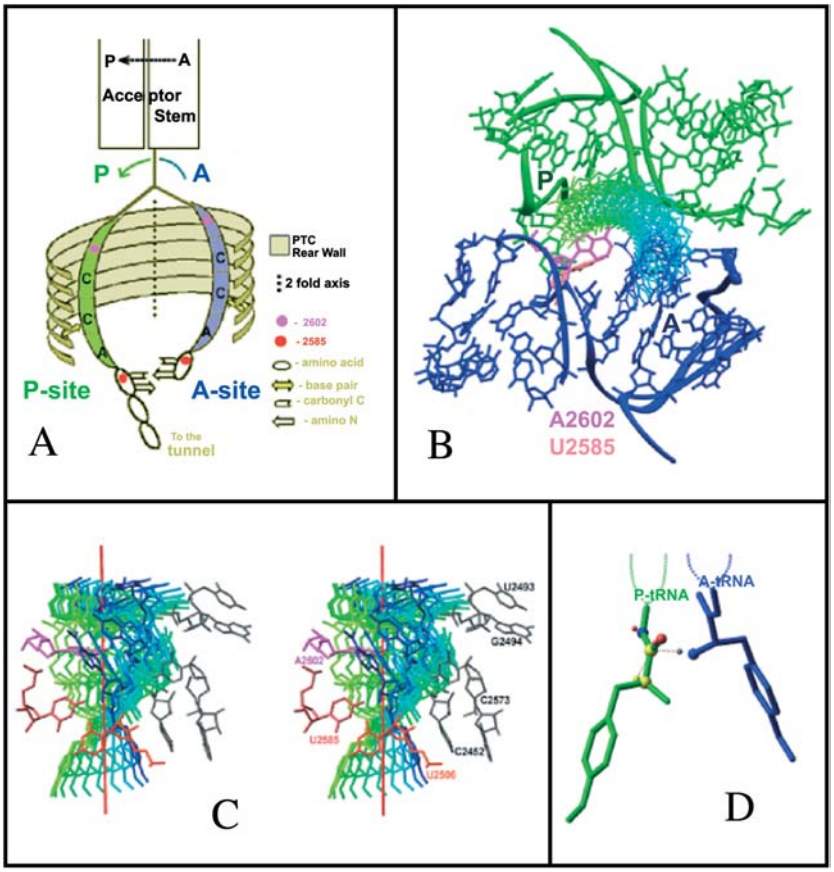

Figure 4 The rotatory motion and its outcome.
(A) Schematic sketch portraying the basic principles of the rotatory mechanism. The tRNA 3′-ends are represented by banana-shaped objects, divided by dotted lines into the four nucleotides composing them. The rear wall is drawn as ribs. The front wall-anchoring nucleotides, A2602 and U2585, are not shown for clarity, but the location of their interactions with the tRNA 3′-ends are marked by colored circles. (B) Snapshots of intermediate stages in the motion of the CCA from the A- to the P-site, viewed down the axis of rotation. The color code for the symmetry-related region is as in Figure 1A. The two front-wall bulged nucleotides are shown in pink and magenta. Simulation of the spiral motion was performed by rotating the aa-3′-end of ASM in its complex with D50S as a rigid body by 179° and translating it by 2 Å in the direction of the tunnel using the LSQKAB program (Bailey, 1994). The axis around which the rotatory motion takes place approximately coincides with the bond connecting the A-site tRNA 3′-end with its acceptor stem and deviates from the SymR symmetry axis by 7°. (C) A stereo view of snapshots of intermediate stages in the motion of the aa-3′-end from the A- to the P-site, as shown in panel (B), but viewed perpendicular to the axis of rotation, showing the front and rear wall interactions with the RM. (D) Stereochemistry of the proposed nucleophilic attack of the ASM amino group (Bashan et al., 2003a) on the derived carbonyl carbon at the P-site. The intermediate-state conformation is overlapped on the reactants for peptide bond formation. Note that the O3′ of the ASM nucleotide representing A76 is replaced by a nitrogen.

the PTC center. Its dimensions suffice for accommodation of the tRNA 3′-end carrying the amino acid throughout the spiral motion (Figure 1C and 3B). Simulation of this motion from the A- to the P-site (Figure 3B,C) showed that the terminus could undergo a clash-free trajectory within the PTC. While the rotating moiety (RM) progresses within this curved corridor, the tRNA nucleotide in position 73 rotates around itself, since the rotation axis passes through its ribose. It therefore stays at the center of the PTC throughout the entire motion and interacts predominantly with A2602, positioned below it.

C74–A76, carrying the amino acid, slide along the rear wall and interact with it until the spiral path is accomplished. In the initial stage of the rotatory motion (0° rotation), the aa-CCA of the A-site substrate interacts with nucleotides U2506, C2507, U2555, C2573 and G2583, and its C75 is base-paired to G2553. As the rotation proceeds (30°), the base of C2573, which bulges from the mismatch zone of H90 into the PTC (Figure 1C), lies against the rotating C75 and A76 (Figure 3C). After approximately 60° of rotation, the bases of nucleotides G2061 and C2063 contact the rotating amino-acid side chain, while C74 interacts with nucleotides U2492–2494 of H89. The phosphate of G2494 creates a wedge that penetrates into a groove between the rotating C74 and C75 (Figure 4C), suggesting that G2494 phosphate directs the RM into its exact path. This task requires firm positioning, consistent with H89 stabilization by an adjacent A-minor motif (with H39), as well as by nucleotides U2493–2494, which are the only rear-wall nucleotides that form base pairs. At 90–135° of rotation, the phosphate of A2453 interacts with the rotated C75, whereas A2451 and C2452 point their bases parallel to the rotating amino-acid side chain in a non-specific manner, in accordance with the demand for invariance of the mechanism under different amino-acid residue types. Alongside, the ribose rings of A2451 and C2452 fit into an angle created between the sugar and the base of the

rotating A76, probably adding to the guidance provided by the rear wall (Figure 4C). In the last stage (150–179° of rotation) P-site contacts similar to those reported previously (Green et al., 1997; Bocchetta et al., 1998; Nissen et al., 2000; Yusupov et al., 2001) are formed. These include the base pair of C75 with G2251, the interactions of C2063, A2451 and U2585 with A76, and of A2062 with the rotated amino acid.

From the front wall, the bases of A2602 and U2585 bulge into the PTC pocket, in the direction of the two-fold axis (Figures 1C and 4B,C). In the structure of the ASM-D50S complex, the nucleotide in position 73 in the tRNA is located at the center of the PTC. The base of A2602 is placed beneath it, within contact distance of the ribose of A73 throughout the course of the rotation, suggesting that the two nucleotides may move in a correlated manner. Similarly, U2585, placed under A2602 and closer to the tunnel entrance, is located within contact distance of the carbonyl O of the bound amino acid throughout the A- to P-site motion. A2602 exhibits a large variety of conformations in different complexes of the large subunit (Agmon et al., 2003; Bashan et al., 2003a) and U2585 reverses the direction of its base by 180° in a complex of D50S with Synercid® – a synergetic antibiotic agent, of which one part binds to the PTC and the other blocks the protein exit tunnel (Agmon et al., 2004; Harms et al., 2004). The continuous interaction with the RM during translocation, combined with the high conservation and unusual inherent flexibility, suggest a pivotal role for U2585 and A2602. This assignment is consistent with the critical role that A2602 plays in selected steps of protein biosynthesis, such as release of the nascent chain (Polacek et al., 2003). A pivotal role has also been suggested for the absolutely conserved U2506, based on cross-links found between the 23S and the tRNA 3′-end in various translocation states (Wower et al., 2000). Although in D50S the base of this nucleotide is facing the amino and carbonyl groups of the RM during the entire A- to P-site trajectory (Figure 4C), its distant location does not allow its direct participation in peptide bond formation, consistent with recent mutagenesis results (Youngman et al., 2004).

The biochemical findings (Moazed and Noller, 1989) that A2602 can either be protected in the initial stage of the translocation or exhibits enhanced reactivity when the tRNA reaches the P-site on both subunits can be explained by the role and position of A2602. Thus, although only shown biochemically for full-size tRNAs, the mere fact that the base of A2602 is shielded under A73 explains its protection during the preliminary stages of the rotatory motion, while the inevitable detachment of A2602 from the P-site 3′-end, required to accommodate the next incoming amino acid, is in accord with its enhanced reactivity found when the tRNA reaches the P-site on both subunits.

During the A- to P-site translocation, the conformation of the terminus seems to be maintained, and its motion is guided and confined by the rear wall from behind and by the two anchoring nucleotides from the front. This encircling support should ensure proper configuration of the RM at the P-site. The spiral nature of the rotatory motion results in a height difference between the reactants (Figure 4A,C), which appears to be connected with advancement of the nascent peptide towards the tunnel. An additional benefit from the 180° rotation performed at each step of the elongation is the guarantee that subsequent side chains in the nascent peptide point in opposite directions, thus indicating an extended conformation of the chain on its way to the tunnel entrance, but not excluding a later rearrangement.

The main outcome of the spiral rotation of the tRNA terminus is the generation of a configuration of the reactants that is suitable for peptide bond formation (Figure 4D) (Agmon et al., 2003; Bashan et al., 2003a). The proper stereochemistry for peptide bond formation requires that the carbonyl carbon of the last residue in the peptidyl chain bound to the P-site tRNA is positioned somewhat closer to the tunnel entrance than its mate in the A-site, so that it faces the amino N of the A-site tRNA (Figure 4A). This arrangement also dictates the polarity of peptide bond formation on the ribosome, since only the amino N at the A-site can carry out a nucleophilic attack on the carbonyl C at the P-site. Attack of the P-site substrate on the tRNA at the A-site is impossible (Figure 4A,D). The resulting arrangement of the reactants is close to the configuration of the intermediate state in a nucleophilic acyl substitution reaction (Figure 4D). In this reaction, the amino-acid primary amine, acting as the nucleophile, selectively attacks one face of the carbonyl carbon, termed the ‘Re face’. Furthermore, the rotatory motion places both reactants for peptide bond formation, namely the A-site nucleophilic amine and the P-site carbonyl-carbon, at a distance reachable by the O2′ of the P-site tRNA A76, consistent with the participation of the P-site tRNA in the catalysis (Dorner et al., 2002; Weinger et al., 2004), as well as with recent mutagenesis and kinetic findings (Sievers et al., 2004; Youngman et al., 2004). As a consequence of the correct positioning of the reactants, peptide bond formation can take place efficiently, implying that the ribosome not only provides the positional component of the catalysis of peptide bond formation, but also places the reactants so they can perform substrate-mediated chemical catalysis (Weinger et al., 2004).

In short, identifying the linkage between the universal ribosomal symmetry and the substrate binding mode revealed a unified ribosomal machinery for peptide bond formation involving translocation within the PTC and advancement of the nascent peptide chain into its exit tunnel (Agmon et al., 2003; Bashan et al., 2003a). This machinery is consistent with results of biochemical and kinetic studies (Nierhaus et al., 1980; Gregory and Dahlberg, 2004; Sievers et al., 2004; Youngman et al., 2004) proposing that positioning of the reactive groups is the critical factor for catalysis of intact tRNA substrates, but does not exclude assistance from ribosomal or substrate moieties. Hence, it appears that the ribosome offers the frame for correct substrate positioning, as well as the structural means for catalytic contribution of the P-site tRNA 2′-hydroxyl group, as suggested previously (Dorner et al., 2002) and verified recently (Weinger et al., 2004). Thus, the ribosome acts as a polymerase that, in addition to catalysis of peptide bond formation, ensures proper and efficient elongation of nascent protein chains.

Sequence conservation and evolution

The importance of the SymR can be inferred from the high conservation of its sequence and secondary and tertiary structures. The similarity between the 3D arrangement of the SymR in the crystal structures of T70S, D50S and H50S (Figure 1A) is in accordance with the vital common function of this region. The high conservation of the secondary structure of the SymR throughout all kingdoms of life is indicated in the phylogenetic conservation map of a sample of 930 different species from three phylogenetic domains and two organelles (Cannone et al., 2002). This map lists the positions appearing frequently in 23S RNA, namely the nucleotides found in more than 95% of the sequences examined. Out of the 2726 nucleotides in the *E. coli* 23S RNA, excluding the SymR, only 36% are 'frequent', whereas 175 out of 178 (98%) nucleotides of the SymR are categorized as such.

Only three positions in the SymR, all in the vicinity of the H74-H75-H80 junction and more than 30 Å away from the region center, vary among different species. These include: U2068, which bulges out of helix H74 in *E. coli*, but is missing in some species; a nucleotide residing between the first second base pairs of helix H80 (A2291 in H50S) that has no equivalent in *E. coli*; and U2431 and A2432 in the rRNA segment between helices H88 and H74, which are missing in certain species, including H50S. Moreover, only 9% of the 'frequent' nucleotides in 23S RNA (SymR excluded) are over 98% phylogenetically conserved, compared to 35% of the 'frequent' nucleotides in the SymR (Figure 2). Importantly, 75% of the 27 nucleotides lying within 10 Å from the two-fold symmetry axis are highly conserved; of these, seven nucleotides are absolutely conserved. These statistics indicate the extreme conservation shown by the SymR, hence pointing at its fundamental role in protein biosynthesis.

The conservation of specific elements in the PTC can be correlated with the universality of the tRNA 3′-end. While passing from the A-site to the P-site by the rotatory motion of the aminoacylated tRNA 3′-end, the tRNA nucleotide in position 73 stays at the center of the PTC throughout the entire motion and interacts predominantly, through its ribose, with A2602, positioned below it. The involvement of the ribose of the tRNA nucleotide in position 73 in the interaction with the PTC is consistent with the lack of conservation of this nucleotide, in contrast to the universal conservation of nucleotides C74–A76 of the tRNA 3′-end (CCA). Absolute conservation of the tRNA A76 seems to originate from tRNA synthetase requirements (Fujiwara et al., 1996), whereas the two cytosines in tRNA 3′-termini are consistent with the universally conserved guanines of the P-loop. These two conserved guanines create two base pairs with the P-site tRNA (G2251 and G2252 with tRNA C75 and C74, respectively) that can direct the conformation of the initial tRNA, thus initiating the rotatory process (Agmon et al., 2004; Baram and Yonath, 2005). One of these base pairs has a symmetrical mate at the A-site (G2553 with tRNA C75), which appears to assist the overall positioning of the tRNA at this site (Yonath, 2003b). Importantly, all three guanines of D50S PTC can form base pairs with the tRNA substrates. In addition to the universal A-site base pair, C75 of the derived P-site terminus is readily base-paired to its counterpart, and P-site C74 requires a minor rearrangement for its participation in base-pairing.

Similarly, the central role of the PTC rear wall is also demonstrated by the extreme conservation of its nucleotides. While the majority of the nucleotides within 10 Å of the symmetry axis passing through the center of the PTC are highly conserved, only seven of them are 100% conserved, of which four are located in the rear wall of the PTC. These are G2061, A2451, C2452 and C2573, which interact with the rotating tRNA aa-3′-end through their bases. In contrast, A2453 and U2493-4, the rear-wall nucleotides whose ribose or phosphate interacts with the rotating tRNA aa-3′-end, are significantly less conserved, in accordance with the involvement of their backbone in the interactions with the RM.

The PTC two-fold symmetry evokes the suggestion that the catalytic site of the ribosome evolved by gene fusion of two separate domains of similar three-dimensional structures. The relatively low level of sequence identity within this symmetrical region may demonstrate that the rigorous requirements for placement of the two reactants in stereochemistry supporting peptide bond formation dictate the preservation of the three-dimensional structure of ribosomal features facilitating substrate placement, regardless of the sequence. This is similar to the conservation of the three-dimensional structure of L16, the only ribosomal protein involved in tRNA positioning (Agmon et al., 2003; Bashan et al., 2003a), despite the low level of sequence homology that has been retained through evolution (Harms et al., 2001), similar to the phenomenon observed first for the globin family (Aronson et al., 1994).

Conclusions

The analysis presented here indicates that the prerequisite for the elaborated process of peptidyl transferase is the positioning of the substrates of this reaction, the A- and P-site tRNA aa-3′-ends, in a stereochemistry favorable for peptide bond formation. The requirement to host the reactants facing each other dictates a ribosomal frame that possesses two-fold symmetry for orienting the reactants, which, together with the specific characteristics of the PTC rear wall, imposes the rotatory mechanism. Specific deviations from the two-fold symmetry are essential for ensuring efficient and smooth processing of peptide bond formation, as well as for the function of the ribosome as an amino acid polymerase. Bulged nucleotides within the SymR, which deviate from the symmetry, seem to stabilize its overall structure and to anchor and provide the exact pattern for the A- to P-site passage, performed by means of a rotatory mechanism. This mechanism is the main element of the unified machinery for peptide bond formation, translocation within the PTC and the advance of nascent chains into the exit tunnel. These three functional steps are controlled by the specifically designed PTC architecture that positions the substrate at appropriate stereochemistry for amino acid

polymerization and enables substrate-mediated chemical catalysis.

Acknowledgments

Thanks are due to Chaim Gilon, Silvio Biali, Miriam Karni, Noam Adir, Remo Rohs, Dan Tawfik and Anthony J. Kirby for valuable discussions, as well as all members of the ribosome group at the Weizmann Institute, especially Maggie Kessler, for constant assistance. X-Ray diffraction data were collected at ID19/SBC/APS/ANL and ID14/ESRF-EMBL. The US National Institutes of Health (GM34360), the Human Frontier Science Program Organization (HFSP RGP0076/2003), and the Kimmelman Center for Macromolecular Assemblies provided support. A.Y. holds the Martin and Helen Kimmel Professorial Chair.

References

Agmon, I., Auerbach, T., Baram, D., Bartels, H., Bashan, A., Berisio, R., Fucini, P., Hansen, H.A., Harms, J., Kessler, M., et al. (2003). On peptide bond formation, translocation, nascent protein progression and the regulatory properties of ribosomes. Eur. J. Biochem. *270*, 2543–3556.

Agmon, I., Amit, M., Auerbach, T., Bashan, A., Baram, D., Bartels, H., Berisio, R., Greenberg, I., Harms, J., Hansen, H.A.S., et al. (2004). Ribosomal crystallography: a flexible nucleotide anchoring tRNA translocation facilitates peptide bond formation, chirality discrimination and antibiotics synergism. FEBS Lett. *567*, 20–26.

Agrawal, R.K., Spahn, C.M., Penczek, P., Grassucci, R.A., Nierhaus, K.H., and Frank, J. (2000). Visualization of tRNA movements on the *Escherichia coli* 70S ribosome during the elongation cycle. J. Cell Biol. *150*, 447–460.

Aronson, H.E., Royer, W.E. Jr., and Hendrickson, W.A. (1994). Quantification of tertiary structural conservation despite primary sequence drift in the globin fold. Protein Sci. *3*, 1706–1711.

Bailey, S. (1994). The CCP4 suite – programs for protein crystallography. Acta Crystallogr. D Biol. Crystallogr. *50*, 760–763.

Ban, N., Nissen, P., Hansen, J., Moore, P.B., and Steitz, T.A. (2000). The complete atomic structure of the large ribosomal subunit at 2.4 Å resolution. Science *289*, 905–920.

Baram, D. and Yonath, A. (2005). From peptide-bond formation to cotranslational folding: dynamic, regulatory and evolutionary aspects. FEBS Lett. *579*, 948–954.

Bashan, A., Agmon, I., Zarivach, R., Schluenzen, F., Harms, J., Berisio, R., Bartels, H., Franceschi, F., Auerbach, T., Hansen, H.A.S., et al. (2003a). Structural basis of the ribosomal machinery for peptide bond formation, translocation, and nascent chain progression. Mol. Cell *11*, 91–102.

Bashan, A., Zarivach, R., Schluenzen, F., Agmon, I., Harms, J., Auerbach, T., Baram, D., Berisio, R., Bartels, H., Hansen, H.A., et al. (2003b). Ribosomal crystallography: peptide bond formation and its inhibition. Biopolymers *70*, 19–41.

Bocchetta, M., Xiong, L., and Mankin, A.S. (1998). 23S rRNA positions essential for tRNA binding in ribosomal functional sites. Proc. Natl. Acad. Sci. USA *95*, 3525–3530.

Cannone, J.J., Subramanian, S., Schnare, M.N., Collett, J.R., D'Souza, L.M., Du, Y., Feng, B., Lin, N., Madabusi, L.V., Müller, K.M., et al. (2002). The Comparative RNA Web (CRW) Site: an online database of comparative sequence and structure information for ribosomal, intron, and other RNAs. BMC Bioinformatics *3*, 1–31.

Cooperman, B.S., Wooten, T., Romero, D.P., and Traut, R.R. (1995). Histidine 229 in protein L2 is apparently essential for 50S peptidyl transferase activity. Biochem. Cell Biol. *73*, 1087–1094.

Diedrich, G., Spahn, C.M., Stelzl, U., Schafer, M.A., Wooten, T., Bochkariov, D.E., Cooperman, B.S., Traut, R.R., and Nierhaus, K.H. (2000). Ribosomal protein L2 is involved in the association of the ribosomal subunits, tRNA binding to A and P sites and peptidyl transfer. EMBO J. *19*, 5241–5250.

Dorner, S., Polacek, N., Schulmeister, U., Panuschka, C., and Barta, A. (2002). Molecular aspects of the ribosomal peptidyl transferase. Biochem. Soc. Trans. *30*, 1131–1136.

Fujiwara, S., Lee, S.G., Haruki, M., Kanaya, S., Takagi, M., and Imanaka, T. (1996). Unusual enzyme characteristics of aspartyl-tRNA synthetase from hyperthermophilic archaeon *Pyrococcus* sp. KOD1. FEBS Lett. *394*, 66–70.

Green, R., Samaha, R.R., and Noller, H.F. (1997). Mutations at nucleotides G2251 and U2585 of 23 S rRNA perturb the peptidyl transferase center of the ribosome. J. Mol. Biol. *266*, 40–50.

Gregory, S.T. and Dahlberg, A.E. (2004). Peptide bond formation is all about proximity. Nat. Struct. Mol. Biol. *11*, 586–587.

Hansen, J.L., Schmeing, T.M., Moore, P.B., and Steitz, T.A. (2002). Structural insights into peptide bond formation. Proc. Natl. Acad. Sci. USA *99*, 11670–11675.

Harms, J., Schluenzen, F., Zarivach, R., Bashan, A., Gat, S., Agmon, I., Bartels, H., Franceschi, F., and Yonath, A. (2001). High resolution structure of the large ribosomal subunit from a mesophilic eubacterium. Cell *107*, 679–688.

Harms, J., Schluenzen, F., Fucini, P. Bartels, H., and Yonath, A. (2004). Alterations at the peptidyl transferase center of the ribosome induced by the synergistic action of the streptogramins dalfopristin and quinupristin. BMC Biol. *2*, 1–10

Hausner, T.P., Atmadja, J., and Nierhaus, K.H. (1987). Evidence that the G2661 region of 23S rRNA is located at the ribosomal binding sites of both elongation factors. Biochimie *69*, 911–923.

Kim, D.F. and Green, R. (1999). Base-pairing between 23S rRNA and tRNA in the ribosomal A site. Mol. Cell *4*, 859–864.

Klein, D.J., Moore, P.B., and Steitz, T.A. (2004). The roles of ribosomal proteins in the structure assembly, and evolution of the large ribosomal subunit. J. Mol. Biol. *340*, 141–177.

Moazed, D. and Noller, H.F. (1989). Intermediate states in the movement of transfer RNA in the ribosome. Nature *342*, 142–148.

Moazed, D., Robertson, J.M., and Noller, H.F. (1988). Interaction of elongation factors EF-G and EF-Tu with a conserved loop in 23S RNA. Nature *334*, 362–364.

Mohr, D., Wintermeyer, W., and Rodnina, M.V. (2002). GTPase activation of elongation factors Tu and G on the ribosome. Biochemistry *41*, 12520–12528.

Nierhaus, K.H., Schulze, H., and Cooperman, B.S. (1980). Molecular mechanisms of the ribosomal peptidyl transferase center. Biochem. Int. *1*, 185–192.

Nissen, P., Hansen, J., Ban, N., Moore, P.B., and Steitz, T.A. (2000). The structural basis of ribosome activity in peptide bond synthesis. Science *289*, 920–930.

Nitta, I., Kamada, Y., Noda, H., Ueda, T., and Watanabe, K. (1998). Reconstitution of peptide bond formation with *Escherichia coli* 23S ribosomal RNA domains. Science *281*, 666–669.

Noller, H.F., Hoffarth, V., and Zimniak, L. (1992). Unusual resistance of peptidyl transferase to protein extraction procedures. Science *256*, 1416–1419.

Polacek, N., Gomez, M.J., Ito, K., Xiong, L., Nakamura, Y., and Mankin, A. (2003). The critical role of the universally conserved A2602 of 23S ribosomal RNA in the release of the nascent peptide during translation termination. Mol. Cell *11*, 103–112.

Schluenzen, F., Tocilj, A., Zarivach, R., Harms, J., Gluehmann, M., Janell, D., Bashan, A., Bartels, H., Agmon, I., Franceschi, F., and Yonath, A. (2000). Structure of functionally activated

small ribosomal subunit at 3.3 Å resolution. Cell *102*, 615–623.

Schmeing, T.M., Seila, A.C., Hansen, J.L., Freeborn, B., Soukup, J.K., Scaringe, S.A., Strobel, S.A., Moore, P.B., and Steitz, T.A. (2002). A pre-translocational intermediate in protein synthesis observed in crystals of enzymatically active 50S subunits. Nat. Struct. Biol. *9*, 225–230.

Schmeing, T.M., Moore, P.B., and Steitz, T.A. (2003). Structures of deacylated tRNA mimics bound to the E site of the large ribosomal subunit. RNA *9*, 1345–1352.

Sievers, A., Beringer, M., Rodnina, M.V., and Wolfenden, R. (2004). The ribosome as an entropy trap. Proc. Natl. Acad. Sci. USA *101*, 7897–7901.

Simonson, A.B. and Lake, J.A. (2002). The transorientation hypothesis for codon recognition during protein synthesis. Nature *416*, 281–285.

Stade, K., Junke, N., and Brimacombe, R. (1995). Mapping the path of the nascent peptide chain through the 23S RNA in the 50S ribosomal subunit. Nucleic Acids Res. *23*, 2371–2380.

Stark, H., Orlova, E.V., Rinke-Appel, J., Junke, N., Mueller, F., Rodnina, M., Wintermeyer, W., Brimacombe, R., and van Heel, M. (1997). Arrangement of tRNAs in pre- and posttranslocational ribosomes revealed by electron cryomicroscopy. Cell *88*, 19–28.

Stark, H., Rodnina, M.V., Wieden, H.J., Zemlin, F., Wintermeyer, W., and Van Heel, M. (2002). Ribosome interactions of aminoacyl-tRNA and elongation factor Tu in the codon-recognition complex. Nat. Struct. Biol. *9*, 849–854.

Uhlein, M., Weglohner, W., Urlaub, H., and Wittmann-Liebold, B. (1998). Functional implications of ribosomal protein L2 in protein biosynthesis as shown by *in vivo* replacement studies. Biochem. J. *331*, 423–430.

Valle, M., Sengupta, J., Swami, N.K., Grassucci, R.A., Burkhardt, N., Nierhaus, K.H., Agrawal, R.K., and Frank, J. (2002). Cryo-EM reveals an active role for aminoacyl-tRNA in the accommodation process. EMBO J. *21*, 3557–3567.

Weinger, J.S., Parnell, K.M., Dorner, S., Green, R., and Strobel, S.A. (2004). Substrate-assisted catalysis of peptide bond formation by the ribosome. Nat. Struct. Mol. Biol. *11*, 1101–1106.

Wilson, K.S. and Noller, H.F. (1998). Mapping the position of translational elongation factor EF-G in the ribosome by directed hydroxyl radical probing. Cell *92*, 131–139.

Wimberly, B.T., Guymon, R., McCutcheon, J.P., White, S.W., and Ramakrishnan, V. (1999). A detailed view of a ribosomal active site: the structure of the L11- RNA complex. Cell *97*, 491–502.

Wimberly, B.T., Brodersen, D.E., Clemons Jr. W.M., Morgan-Warren, R.J., Carter, A.P., Vonrhein, C., Hartsch, T., and Ramakrishnan, V. (2000). Structure of the 30S ribosomal subunit. Nature *407*, 327–339.

Wower, J., Kirillov, S.V., Wower, I.K., Guven, S., Hixson, S.S., and Zimmermann, R.A. (2000). Transit of tRNA through the *Escherichia coli* ribosome. Cross-linking of the 3′-end of tRNA to specific nucleotides of the 23 S ribosomal RNA at the A, P, and E sites. J. Biol. Chem. *275*, 37887–37894.

Wriggers, W., Agrawal, R.K., Drew, D.L., McCammon, A., and Frank, J. (2000). Domain motions of EF-G bound to the 70S ribosome: insights from a hand-shaking between multi-resolution structures. Biophys. J. *79*, 1670–1678.

Yonath, A. (2003a). Structural insight into functional aspects of ribosomal RNA targeting. ChemBioChem *4*, 1008–1017.

Yonath, A. (2003b). Ribosomal tolerance and peptide bond formation. Biol. Chem. *384*, 1411–1419.

Youngman, E.M., Brunelle, J.L., Kochaniak, A.B., and Green, R. (2004). The active site of the ribosome is composed of two layers of conserved nucleotides with distinct roles in peptide bond formation and peptide release. Cell *117*, 589–599.

Yusupov, M.M., Yusupova, G.Z., Baucom, A., Lieberman, K., Earnest, T.N., Cate, J.H., and Noller, H.F. (2001). Crystal structure of the ribosome at 5.5 Å resolution. Science *292*, 883–896.

Zarivach, R., Bashan, A., Berisio, R., Harms, J., Auerbach, T., Schluenzen, F., Bartels, H., Baram, D., Pyetan, E., Sittner, A. et al. (2004). Functional aspects of ribosomal architecture: symmetry, chirality and regulation. J. Phys. Org. Chem. *17*, 901–912.